Raman and ATR Infrared Spectra of Gypsum Crystallization Water

DOI: 10.2139/ssrn.4975648

Raman and ATR Infrared Spectra of Gypsum Crystallization Water

Amelia Carolina Sparavigna

Department of Applied Science and Technology, Polytechnic University of Turin, Italy

Abstract: Here we propose a comparison of Raman and Attenuated Total Reflectance (ATR) Infrared spectra of the gypsum crystallization water. The comparison is obtained by means of some deconvolutions of the OH-stretching mode spectral regions, where the vibrations of the water molecules bonded into gypsum crystal structure are evidenced. We use gypsum Raman and ATR-IR spectra available from RRUFF database. For what is regarding the data from literature, we will refer also to those obtained by research in the first period of the Raman spectroscopy, that is for 1929 to 1945. We find good agreement among data.

Keywords: Raman spectroscopy, ATR Infrared spectroscopy, q-Gaussian functions, q-BWF functions, Hydroxyl-stretching Raman region, OH-stretching Raman region.

Introduction

Recently, we have considered the detection of water by means of Raman spectroscopy in the cases of minerals of vivianite and natrolite groups. We used for these previous investigations the RRUFF database and the Raman broad scans therein. To deconvolute the spectra, we applied the q-Gaussian profiles (see Appendix). In the RRUFF database, we can find also the spectra from ATR infrared spectroscopy, "one of the most commonly used sampling techniques in recent times" (Subramanian & Rodriguez-Saona, 2009). As previously discussed in an analysis of barite-group and carbonate minerals, the ATR bands appear being asymmetrical (Kendix, 2009), and therefore, for the deconvolution of the spectrum, an asymmetric band shape is required. Using the asymmetric q-BWF functions (Sparavigna, 2023), we can determine the components of ATR-IR spectra and compare with infrared data available from literature, as we made for barite and carbonate materials (Sparavigna, 2024). Previously, we have applied the q-BWF functions to the Raman bands of molybdenum disulfide and barium titanate (link1, link2).

Here we analyze Raman and ATR-infrared spectra, available from RRUFF database, of the gypsum crystallization water. This crystallization water has been already considered by us, but here we want to stress the deconvolution of the ATR-infrared bands with q-Gaussian and q-BWF functions. The q-Gaussian functions have been proposed for the deconvolution of Raman spectra for the first time by Sparavigna, 2023; the q-BWF (q-Breit-Wigner-Fano) functions have been defined by Sparavigna in 2023. For the Raman spectroscopy on gypsum, we will use also the Raman data obtained by researchers in the first period of the Raman spectroscopy, that is for 1929 to 1945. We find good agreement among data.

Gypsum

Gypsum is an ionic crystal, which has its unit cell containing four molecules of $CaSO_4.2H_2O$. It was a mineral investigated as soon as the Raman effect had been discovered. In Saksena, 1941, Table III, we can find given the Raman shifts published by the previous literature, listed along with the data observed by Saksena. We can find the values of the ν_1, ν_2, ν_3 and ν_4 Raman frequencies of the SO_4 ion (see Saksena, 1941). "The presence of two water-bands at 3406 and 3493 [cm^{-1}] is well established. [Saksena] has been unable to confirm neither the presence of a third band at 3240 reported by [K.S.] Krishnan (1929) nor the splitting observed by Rasetti (1932) for the band 3406". The following Table is like that given by Saksena, 1941 (see please references therein). Kariamanikkam

Srinivasa Krishnan's paper is "The Raman spectra of crystals", Indian J. Phys. 4, 131-138(1929). This was the last article by K. S. Krishnan on Raman spectroscopy. Let us stress that K. S. Krishnan discovered with Chandrasekhara Venkata Raman the Raman effect.

Table I: Gypsum Raman shift (cm^{-1}), from Saksena, 1941, and references therein. Note the data 3426 from Rasetti (1932). According to R. S. Krishnan, 1945, the value is 3476, as "obtained from measurements made on the photographs reproduced in Rasetti's paper. The value given by Rasetti (1932) for this band is 3426 which should evidently be wrong".

Krishnan (1929)	3240	3397	3493
Nisi (1931)		3404	3497
Cabannes (1932, 1938)		3404	3495
Rasetti (1932)		3399	3426
Saksena (1941)		3406	3493

Note that three bands are present in the spectrum of water for sure, therefore the data from K. S. Krishnan, 1929, are very interesting.

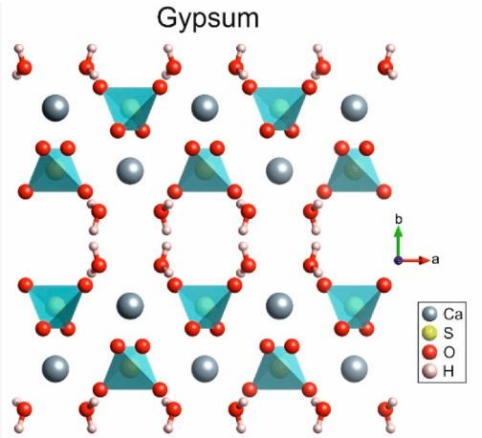

Fig.1. Gypsum lattice as given in the Fig.1 by Schmid et al., 2020, CC BY license (http://creativecommons.org/licenses/by/4.0/).

Crystallization water and Raman bands

Rappal Sangameswaran Krishnan, in 1945, proposed a new study on gypsum. He used the mercury resonance radiation λ2536.5 for exciting the Raman spectrum. In Krishnan's article we can find an interesting comparison regarding the spectrum of the crystallization water, that here we propose in the following Table.

Table II: Raman shift (cm^{-1}) as in R. S. Krishnan, 1945.

Gypsum	3258 3334	3406 3495	3606 3680
Water	3231	3436	3605
Ice at 0°C	3193	3391	3549

The correspondence evidenced by Krishnan "follows as a natural consequence of the fact that in gypsum the water molecules are concentrated in separate sheets which are only loosely bound with other sheets of ions and as such the oscillations of the water molecules are not appreciably modified in the crystalline state" (Krishnan, 1945). The gypsum crystal structure is shown in our Fig.1, and in Yu et al., 2016, according to Chen, 2006. "The bands in gypsum are very much sharper than those observed with ordinary water and consequently their maxima could be measured with a high degree of accuracy. The spectrum of gypsum shows another interesting feature. *The three principal water bands are split into six fairly narrow bands.* They form three pairs as shown [here in the previously given table]. The difference in the frequency shifts of the two components of each pair is

approximately constant for the three pairs, … Results obtained by Cabannes (1938), Saksena (1941) and Rao (1941) from polarisation studies indicate that the band at 3406 belongs to the symmetric class, while the one at 3495 to antisymmetric class. Similar behavior should be exhibited by the other two pairs of bands also. Because of the antisymmetric nature of the band at 3495 cm^{-1} Cabannes (1938) had suggested that this band should correspond to the Raman inactive valence vibration of the H_2O molecule, which was rendered active in the crystalline environment" (Krishnan, 1945, and references therein). "The Raman bands of water in several crystalline hydrates have been the subject of study by numerous investigators" (see references in Krishnan, 1945). Regarding the experiment, we find that the spectrum of the water of crystallization in gypsum, as obtained by Roop Kishore (1942) and Krishnan, "shows far greater detail than any recorded by others not only in gypsum but in other crystalline hydrates as well. The success is due to the use of the intense *mercury resonance radiation* for exciting the Raman spectrum" (Krishnan, 1945).

In our previous discussion about the gypsum crystallization water, we considered the spectra available in RRUFF database (Lafuente et al., 2015). We have two available scans, the R040029 and R060509 broad scans, with unoriented samples and instrument setting Thermo Almega XR 532nm at 100% of 150 mW. We use data in the range from 3000 to 4000 cm^{-1}. A spline baseline adjustment was applied. As shown in the Figure 2, we used a deconvolution with q-Gaussian functions.

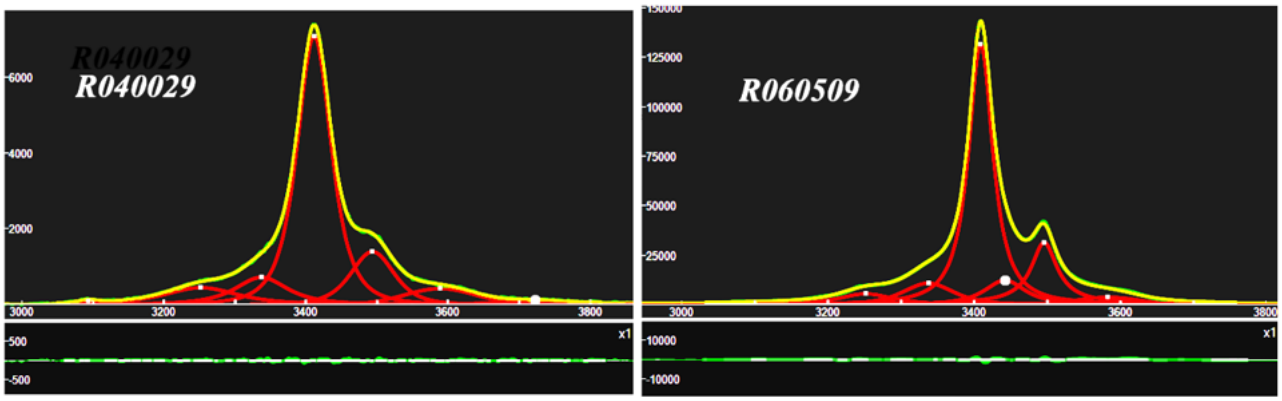

Fig.2: Deconvolution of gypsum RRUFF R040029 (left) and RRUFF R060509 (right) spectra. The region of the crystallization water is decomposed into seven and six q-Gaussian bands (red curves) respectively. The lower part of the images is showing the misfit, that is the difference between data (green) and the sum of components (yellow curve). R040029: the centers of components are at 3093, 3252, 3338, 3411, 3493, 3589, 3722 cm^{-1}. R060509: the centers of components are at 3252, 3337, 3409, 3496, 3583 cm^{-1}.

The plots in the Fig.2 have been obtained by means of software Fityk (Wojdyr, 2010), after defining in it the q-Gaussian functions (see Appendix A for further details). By means of the data obtained from q-Gaussian deconvolution, we can compare the Raman shift (cm^{-1}) of the centers of components given in the Figure 1, with the results given in Krishnan, 1945. It is admirable the agreement. The main peak is at 3406-3411 cm^{-1}, according to Krishnan, 1945. Here in the following table, the comparison is shown (centers of components given in cm^{-1}).

Table III: Raman shift (cm^{-1}) as in our Fig.2 and in R. S. Krishnan, 1945.

Gypsum (Krishnan)		3258	3334	3406	3495	3606	3680
R040029	3093	3252	3338	3411	3493	3589	3722
R060509		3252	3337	3409	3496	3583	

In 1945, we can find evidenced by the spectroscopy on gypsum a strong enhancement of the Raman technique. In fact, Rappal Sangameswaran Krishnan improved his Raman spectroscopy by using the "Rasetti technique". Franco Rasetti was a physicist that, with Enrico Fermi, discovered the key processes to obtain nuclear fission. In 1930, he was appointed to the chair in spectroscopy at the University of Rome. It was in 1929, that Rasetti proposed his new approach to Raman spectroscopy. "We owe to Rasetti (1929, 1930) the development of a remarkably useful technique for the study of the Raman effect, the value of which has been demonstrated by the resounding success with which he himself applied it in several cases of fundamental interest" (Krishnan, 1943). A detailed discussion of Rasetti's technique is available in Krishnan, 1943, and also in his article about calcite, 1945. In his article on gypsum, we can find told that also Roop Kishore (1942), "using *the Rasetti technique"* was able of finding "three more weak water bands with mean frequency shifts 3244, 3309 and 3584 cm^{-1} in the neighborhood of the two principal water bands" (Krishnan, 1945). Then, let us add Kishore's results to our previous table for comparison.

Table IV: Raman shift (cm^{-1}) as in our Fig.2, in R. S. Krishnan, 1945, and Kishore, 1942.

Gypsum (Krishnan)		3258	3334	3406	3495	3606	3680
R040029	3093	3252	3338	3411	3493	3589	3722
R060509		3252	3337	3409	3496	3583	
Gypsum (Kishore)		3244	3309	3410	3480	3584	

Also in Kishore, 1942, we find given details about Rasetti method, referring to his work of 1932.

ATR Infrared spectrum

For sample RRUFF Gypsum R040029 we have the Attenuated Total Reflectance Infrared spectrum. We concentrate on the region oof the crystallization water.

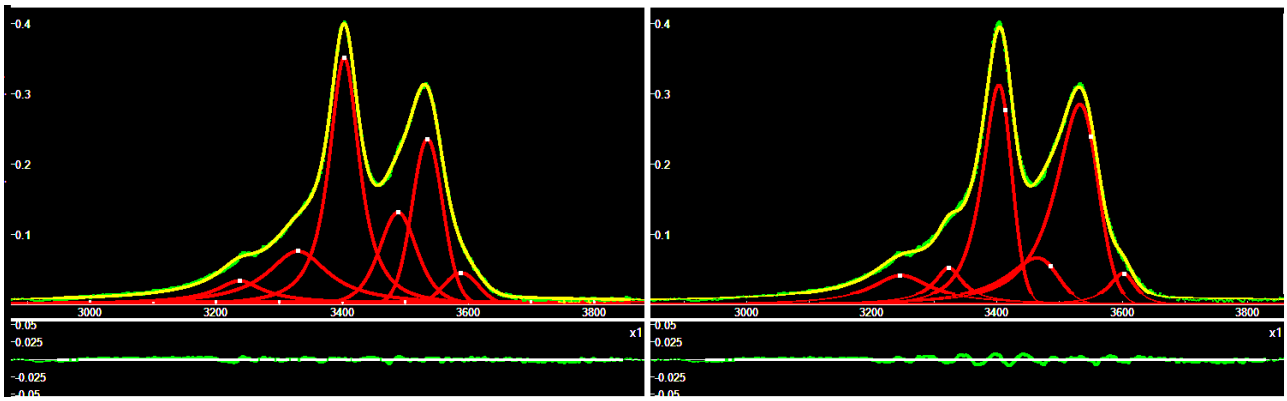

Fig.3: Deconvolution of ATR-IR gypsum RRUFF R040029. On the left, the deconvolution is obtained by means of q-Gaussian functions, on the right by means of q-BWF functions. The region of the crystallization water is decomposed into six bands (red curves). The lower part of the images is showing the misfit, that is the difference between data (green) and the sum of components (yellow curve). R040029 (left, q-Gaussians): the centers of components are at 3237, 3329, 3403, 3489, 3535, 3589 cm^{-1}. R040029 (right, q-BWFs): the peaks of components are at 3246, 3323, 3404, 3465, 3535, 3602 cm^{-1}. Note that, being asymmetric, the center of a q-BWF function does not coincide with its peak.

The following Table is illustrating a further comparison, among the Raman data previously reported, the ATR-IR data here determined, and other infrared data. The agreement seems being good.

Table V: Raman and IR data (cm^{-1}).

Krishnan, K. S. (Raman)		3240		3397	3493				
Hisamitu Nisi (Raman)				3404	3497				
Cabannes (Raman)				3404	3495				
Rasetti (Raman)				3399	3476				
Saksena (Raman)				3406	3493				
Dickinson & Dillon (Raman)				3403	3491.5				
Narayana Rao (Raman)				3405	3489				
Anbalagan et al. (Raman)				3404	3500				
Kishore (Raman)		3244	3309	3410	3480			3584	
Krishnan, R.S. (Raman)		3258	3334	3406	3495			3606	3680
R060509 (Raman)		3252	3337	3409	3496			3583	
R040029 (Raman)	3093	3252	3338	3411	3493			3589	3722
R040029 (ATR, q-Gaussians)		3237	3329	3403	3489		3535	3589	
R040029 (ATR, q-BWFs)		3246	3323	3404	3465		3535	3602	
Chukanov (Transmitt.)		3230		3395			3540		
Univ. Tartu (ATR-FT-IR)		3242		3402		3526			
Shillito et al. (Transmitt.)		3240		3394	3456	3510	3548		
Seidl et al., Fig.2		3242		3404	3496		3549		
Seidl et al., Fig.3		3246		3407	3495		3550		
Al Dabbas et al., Fig.4		3235		3404	3495		3547		
Anbalagan et al., infrared				3400			3541		

For sample R040029, we can see that a shift of values seems being existing between Raman and ATR-IR data. It is therefore necessary to add a short discussion about ATR-IR technique, which is a method based on the internal reflectance phenomenon. When an IR light beam passes from a medium with a high refractive index into "a medium of low refractive index (sample)", we can observe that "at a particular angle of incidence, almost all the light waves are reflected back. This phenomenon is called total internal reflection. In this condition, some amount of the light energy escapes the crystal and extends a small distance (0.1–5 μm) beyond the surface in the form of waves" (Subramanian & Rodriguez-Saona, 2009). The waves are evanescent waves. "The intensity of the reflected light reduces at this point. This phenomenon is called *attenuated total reflectance*" (Subramanian & Rodriguez-Saona, 2009).

"The partial penetration of the IR light by an evanescent wave allows an absorption spectrum to be recorded" (see for instance, QD-Europe). The penetration depth of the evanescent wave is a function of the angle of incidence at the sample surface interface. "Deeper penetration into a sample is achieved with either a smaller incident angle or a lower refractive index ATR crystal" (QD-Europe). An ATR spectrum is "different to that obtained for the same sample when collected as a transmission spectrum" since measurement methods are different, being differences dictated "by the fundamental way the sample information is being collected". In transmission spectroscopy, the light passes through the sample, "whereas ATR spectroscopy is the interaction of light by passage into the surface of a sample species. *Note that neither method can be regarded as giving the "correct" spectrum – they are simply different*" (QD-Europe). The web site details the role of wavelength and refractive index on the penetration depth of the light. Moreover, the differences of intensities, the band shift, and the band asymmetries that we observe when an ATR spectrum is compared to a transmission spectrum, are discussed. For instance, regarding the band distortion, it is told that "sometimes in ATR measurements the absorption bands can become *slightly asymmetric* compared to the bands seen in

transmission measurements" (QD-Europe). The deformation of the band shape is due to "the rapid change of refractive index of the sample across the band". "The refractive index of the sample varies from a low value on the short wavelength side of the band to a high value on the long wavelength side. This causes the effective penetration depth to also rapidly increase toward the long wavelength side and causes the characteristic shape of the bands seen" (QD-Europe).
About data comparison, let us consider also the observations made by Kendix, 2009: "in most cases comparison of standard spectra collected in FIR transmission and FIR ATR mode leads to only a few differences. The most obvious, when comparing transmission with ATR, is the distortion of band shape. The ATR band shape appears *asymmetrical* in the lower wavenumber region when compared to spectra collected in transmission mode. Also, *intensity differences* are noticed. However, the biggest difference can be the *shift* of strong absorbing bands moving to lower wavenumbers in ATR mode" (Kendix, 2009). Usually, "the shifts observed are small, approximately 1-10 cm^{-1}, but for very strong absorbing compounds the shifts observed can be as big as 30-50 cm^{-1}" (Kendix, 2009). Then the ATR spectra can be "considerably different from transmission spectra with respect to intensities, band shift and band distortions" (Kendix, 2009).

Appendix: q-Gaussian and q-BWF functions

The fitting of Raman spectra with q-Gaussian line shapes has been proposed for the first time in 2023 by A. C. Sparavigna. The q-Gaussian line shape is a function based on the Tsallis q-form of the exponential function (Tsallis, 1988). This exponential form is characterized by a q-parameter. When q is equal to 2, we have the Lorentzian function. If q is close to 1, we have a Gaussian function. For values of q between 1 and 2, we have a bell-shaped symmetric function with power-law wings ranging from Gaussian to Lorentzian tails. As shown on many occasions, the q-Gaussians are suitable for fitting Raman spectra (from examples proposed in SSRN to the SERS cases, for instance). However, we can define also an asymmetric function, turning the Breit-Wigner-Fano (BWF) into a q-BWF function (Sparavigna, 2023). Let us write the BWF as follow:

$$\mathrm{BWF}(x) = C\frac{\left[1-\xi\gamma^{1/2}(x-x_o)\right]^2}{[1+\gamma(x-x_o)^2]}$$

In the function given above, x_o represents the center of the line. When asymmetry parameter ξ is zero, BWF becomes a symmetric Lorentzian function. Note that the center of the line does not correspond to the position of the peak of the function (Ferrari & Robertson, 2000). As in Sparavigna, 2023, we can define the q-BWF function in the following manner:

$$\text{q-BWF} = C\left[1-\xi\gamma^{1/2}(q-1)^{1/2}(x-x_o)\right]^2[1+(q-1)\gamma(x-x_o)^2]^{1/(1-q)}$$

In fact, the Lorentzian function is substituted by a q-Gaussian function. The q-Gaussian is given as $f(x) = Ce_q(-\gamma x^2)$, where $e_q(.)$ is the q-exponential function and C a scale constant (Hanel et al., 2009). The q-exponential has expression: $e_q(u) = [1+(1-q)u]^{1/(1-q)}$. For spectroscopy, we write the q-Gaussian function with the center of the band at x_o:

$$q\text{-}Gaussian = Cexp_q(-\gamma(x-x_o)^2) = C\,[1+(q-1)\gamma(x-x_o)^2]^{1/(1-q)}.$$

We can apply q-Gaussian and q-BWF functions by means of Fityk software. In Fityk, a q-Gaussian function can be defined in the following manner:

define Qgau(height, center, hwhm, q=1.5) = height*(1+(q-1)*((x-center)/hwhm)^2)^(1/(1-q)),

where q=1.5 is the initial guessed value of the q-parameter. Parameter hwhm is the half width at half maximum of the line. When q=2, the q-Gaussian is a Lorentzian function, that we can find defined in Fityk as:

Lorentzian(height, center, hwhm) = height/(1+((x-center)/hwhm)^2).

When q is close to 1, the q-Gaussian becomes a Gaussian function.
The q-Breit-Wigner-Fano (q-BWF) can be defined as:

Qbreit(height, center, hwhm, q=1.5, xi=0.1) = (1-xi*(q-1)*(x-center)/hwhm)^2 * height*(1+(q-1)^0.5 *((x-center)/hwhm)^2)^(1/(1-q)).

And the BWF can be defined as:

Breit(height, center, hwhm, xi=0.1) = (1-xi*(x-center)/hwhm)^2 * height/(1+((x-center)/hwhm)^2).

Using +xi instead of -xi does not change the fitting results in Fityk.

References

1. Al Dabbas, M., Eisa, M. Y., & Kadhim, W. H. (2014). Estimation of gypsum-calcite percentages using a Fourier transform infrared spectrophotometer (FTIR), in Alexandria Gypsiferous Soil-Iraq. Iraqi Journal of Science, 1916-1926.
2. Anbalagan, G., Mukundakumari, S., Murugesan, K. S., & Gunasekaran, S. (2009). Infrared, optical absorption, and EPR spectroscopic studies on natural gypsum. Vibrational Spectroscopy, 50(2), 226-230.
3. Cabannes, J. (1932). The Raman spectrum of the sulfate in gypsum. Comptes rendus hebdomadaires des séances de l'Académie des sciences, 195, 1353-1355.
4. Chen, P. (2006) Crystal mineralogy [M]. Chemical Industry Press, Beijing.
5. Chukanov, N.V. (2014). IR Spectra of Minerals and Reference Samples Data. Springer Geochemistry/Mineralogy. Springer, Dordrecht. doi:10.1007/978-94-007-7128-4_2
6. Dickinson, R. G., & Dillon, R. T. (1929). The Raman spectrum of gypsum. Proceedings of the National Academy of Sciences, 15(9), 695-699.
7. Ferrari, A. C., & Robertson, J. (2000). Interpretation of Raman spectra of disordered and
8. amorphous carbon. Physical Review B 61: 14095–14107.
9. Hanel, R., Thurner, S., & Tsallis, C. (2009). Limit distributions of scale-invariant probabilistic models of correlated random variables with the q-Gaussian as an explicit example. The European Physical Journal B, 72(2), 263.
10. Kendix, E. L. (2009). Transmission and Reflection (ATR) Far-Infrared Spectroscopy Applied in the Analysis of Cultural Heritage Materials. Ph.D. Thesis, Alma Mater Studiorum Università di Bologna, Bologna, Italy.
11. Kishore, R. (1942, July). Raman spectra of crystals excited by the mercury resonance radiations. In Proceedings of the Indian Academy of Sciences-Section A (Vol. 16, No. 1, p. 36). New Delhi: Springer India.
12. Krishnan, K. S. (1929). The Raman spectra of crystals, Indian J. Phys. 4, 131-138.
13. Krishnan, R. S. (1943, November). Raman spectra of crystals and their interpretation. In Proceedings of the Indian Academy of Sciences-Section A (Vol. 18, pp. 298-308). Springer India.

14. Krishnan, R. S. (1945, September). Raman spectra of the second order in crystals: Part I: Calcite. In Proceedings of the Indian Academy of Sciences-Section A (Vol. 22, No. 3, p. 182). New Delhi: Springer India.
15. Krishnan, R. S. (1945, October). Raman spectra of the second order in crystals: Part II. Gypsum. In Proceedings of the Indian Academy of Sciences-Section A (Vol. 22, pp. 274-283). Springer India.
16. Lafuente, B., Downs, R. T., Yang, H., & Stone, N. (2015). 1. The power of databases: The RRUFF project. In Highlights in mineralogical crystallography (pp. 1-30). De Gruyter (O).
17. Narayana Rao, D. A. A. S. (1941, February). Raman effect in gypsum. In Proceedings of the Indian Academy of Sciences-Section A (Vol. 13, pp. 137-149). Springer India.
18. Raman, C. V., & Krishnan, K. S. (1928). A new type of secondary radiation. Nature, 121(3048), 501-502.
19. Raman, C. V., & Krishnan, K. S. (1929). The production of new radiations by light scattering. - Part I. Proceedings of the Royal Society of London. Series A, Containing Papers of a Mathematical and Physical Character, 122(789), 23-35.
20. Rasetti, F. (1929). Incoherent scattered radiation in diatomic molecules. Physical Review, 34(2), 367
21. Rasetti, F. (1931). Raman Spectra of Crystals, Nature, 127(3208), 626-627.
22. Rasetti, F. (1932). Sopra l'effetto Raman nei cristalli. Il Nuovo Cimento (1924-1942), 9(3), 72-75.
23. Saksena, B. D. (1941, January). Raman spectrum of gypsum. In Proceedings of the Indian Academy of Sciences-Section A (Vol. 13, No. 1, pp. 25-32). New Delhi: Springer India.
24. Schmid, T., Jungnickel, R., & Dariz, P. (2020). Insights into the CaSO4–H2O system: A Raman-spectroscopic study. Minerals, 10(2), 115.
25. Seidl, V., Knop, O., & Falk, M. (1969). Infrared studies of water in crystalline hydrates: gypsum, CaSO4• 2H2O. Canadian Journal of Chemistry, 47(8), 1361-1368.
26. Shillito, L. M., Almond, M. J., Nicholson, J., Pantos, M., & Matthews, W. (2009). Rapid characterisation of archaeological midden components using FT-IR spectroscopy, SEM–EDX and micro-XRD. Spectrochimica Acta Part A: Molecular and Biomolecular Spectroscopy, 73(1), 133-139.
27. Sparavigna, A. C. (2023). q-Gaussian Tsallis Line Shapes and Raman Spectral Bands. Int. J. Sciences, 12(3), 27-40.
28. Sparavigna, A. C. (2023). Asymmetric q-Gaussian functions generalizing the Breit-Wigner-Fano functions. Zenodo. https://doi.org/10.5281/zenodo.8356165
29. Sparavigna, A. C. (2024). Hydroxyl-Stretching Region in the Raman Broad Scans on Minerals of the Vivianite Group (Vivianite, Baricite, Bobierrite, Annabergite, Erythrite). Int. J. Sciences, 13(08), 23-36.
30. Sparavigna, A. C. (2024). Water in zeolites of natrolite group and its OH-stretching region in Raman spectroscopy. ChemRxiv. https://doi.org/10.26434/chemrxiv-2024-wdv4b
31. Sparavigna, A. C. (2024). q-BWF functions to deconvolute the attenuated total reflectance infrared spectra of the barite-group minerals. ChemRxiv, https://doi.org/10.26434/chemrxiv-2024-9x1jz
32. Sparavigna, A. C. (2024). Gypsum Crystallization Water: Comparing a Laser Excited Raman Spectrum with a Mercury Resonance Radiation Excited Spectrum (Rasetti Technique). International Journal of Sciences, 13(09), 42-49. http://dx.doi.org/10.18483/ijSci.2798

33. Sparavigna, A. C. (2024). Attenuated Total Reflectance Infrared Spectra of Carbonate Minerals, Deconvoluted by Means of q-BWF Functions. International Journal of Sciences, 13(09), 76-83. http://dx.doi.org/10.18483/ijSci.2803
34. Subramanian, A., & Rodriguez-Saona, L. (2009). Chapter 7-Fourier Transform Infrared (FTIR) Spectroscopy, in Infrared Spectroscopy for Food Quality Analysis and Control, D. Sun, Ed.
35. Tsallis, C. (1988). Possible generalization of Boltzmann-Gibbs statistics. Journal of statistical physics, 52, 479-487.
36. Wojdyr, M. (2010). Fityk: a general-purpose peak fitting program. Journal of applied crystallography, 43(5), 1126-1128.
37. Yu, W. D., Liang, W. G., Li, Y. R., & Yu, Y. M. (2016). The meso-mechanism study of gypsum rock weakening in brine solutions. Bulletin of Engineering Geology and the Environment, 75, 359-367.